Hindawi
Shock and Vibration
Volume 2019, Article ID 4509630, 11 pages
https://doi.org/10.1155/2019/4509630

Research Article

Flexural-Torsional Vibration of Thin-Walled Beams Subjected to Combined Initial Axial Load and End Bending Moment: Application to the Design of Saw Tooth Blades

Van Binh Phung,[1] Anh Tuan Nguyen,[1] Hoang Minh Dang,[2] Thanh-Phong Dao,[3,4] and V. N. Duc[5,6]

[1]*Le Quy Don Technical University, Hanoi, Vietnam*
[2]*Industrial University of Ho Chi Minh City, Ho Chi Minh City, Vietnam*
[3]*Division of Computational Mechatronics, Institute for Computational Science, Ton Duc Thang University, Ho Chi Minh City, Vietnam*
[4]*Faculty of Electrical and Electronics Engineering, Ton Duc Thang University, Ho Chi Minh City, Vietnam*
[5]*Division of Construction Computation, Institute for Computational Science, Ton Duc Thang University, Ho Chi Minh City, Vietnam*
[6]*Faculty of Civil Engineering, Ton Duc Thang University, Ho Chi Minh City, Vietnam*

Correspondence should be addressed to V. N. Duc; nguyenvietduc@tdtu.edu.vn

Received 31 July 2019; Revised 9 November 2019; Accepted 3 December 2019; Published 27 December 2019

Academic Editor: Itzhak Green

The present paper analyzes the vibration issue of thin-walled beams under combined initial axial load and end moment in two cases with different boundary conditions, specifically the simply supported-end and the laterally fixed-end boundary conditions. The analytical expressions for the first natural frequencies of thin-walled beams were derived by two methods that are a method based on the existence of the roots theorem of differential equation systems and the Rayleigh method. In particular, the stability boundary of a beam can be determined directly from its first natural frequency expression. The analytical results are in good agreement with those from the finite element analysis software ANSYS Mechanical APDL. The research results obtained here are useful for those creating tooth blade designs of innovative frame saw machines.

1. Introduction

Thin-walled beams are important structural elements that are used widely in civil and mechanical engineering, machinery, aviation, and other areas due to their lightweight feature and the potential to reduce material consumption [1, 2]. Apart from strength and stability, vibration characteristics also must be considered deliberately while studying beams, especially in high-speed vehicle structures [3, 4]. Thin-walled beams are employed in many machine components in various manners. These structures are often subjected to many types of loading simultaneously with different boundary conditions. These boundary conditions in turn cause prestresses, which may alter the vibration characteristics of beam structures. A typical example of this phenomenon can be seen in the case of frame saw machine blades [5].

Currently, there are two main approaches to deal with prestressed thin-walled beam vibration problems. The first is based on finite element methods (FEMs) that solve problems numerically. For thin-walled beams, several typical load cases, including axial loads, eccentric axial loads, and a combination of axial force and bending moment have been studied. It is widely agreed that the first vibration mode, which couples the bending and torsional vibrations, has the greatest influence on the properties of beam structures. Li

et al. [6, 7] used the dynamic transfer matrix method to calculate the natural frequencies of axially loaded thin-walled Timoshenko beams while studying coupled bending-torsional vibration. Banerjee [8] and Banerjee and Williams [9] succeeded in developing explicit expressions for the coupled bending-torsional dynamic stiffness matrix of an axially loaded Timoshenko beam element. Vörös [10] analyzed the coupled bending and torsional vibrations and mode shapes of straight beams induced by initial lateral loads. In particular, while exploring the bending-torsional vibration of beams subjected to axial loads and end moments, Kashani et al. [11] pointed out that end moments tend to have significant effects on the first vibration mode and its natural frequency. Additionally, the influence of the initial in-plane deformations, which are generated by separate initial uniform moments, or distributed loads and/or concentrated loads on the natural frequencies of simply supported thin-walled composite beams was examined by Machado and Cortínez [12]. Vo and Lee [13] determined the interaction curves for the vibration and buckling of simply supported composite box beams subjected to axial loads and end moments. The aforementioned numerical methods are typically used to determine the natural frequencies of a beam under a given loading condition. However, in some cases it is necessary to predict the loads acting on a beam when the natural frequencies are obtained by measurement equipment [14]. For these cases, FEMs are normally inapplicable.

The second approach, which is developed based on analytical tools, has drawn the interest of many researchers due to its ability to express the explicit relationships between the vibration properties and the structural parameters of thin-walled beams. Using this approach, Bokaian [15] and Abramovich [16] studied the natural frequencies of beams under tensile and compressive axial loads, respectively. Moreover, Binici [17] evaluated the vibrations of beams with multiple open cracks under axial force. Busool and Eisenberger [18] explored the effects of constant axial loads on the natural frequencies of uniform multispan beams. In these studies, only single loads were considered. When additional types of loading are included together in a problem, the solution process becomes more complex. Béri et al. [19] assessed the effects of potential energy variations on the natural frequencies of a cantilever beam under compression and lateral forces. Suryanarayan and Joshi [20] scrutinized the coupled bending and torsional vibration of an eccentrically stretched strip. Nevertheless, the formulae pertaining to the natural frequencies obtained in their work can only be used for either the loading system under axial tension (or compression) or that under an eccentric axial load. Dokumaci [21] analyzed the coupled bending and torsion vibration characteristics of uniform beams; however, the expressions derived in that study are not efficient for practical applications. Among the studies described above, it is noteworthy that the vibration of thin-walled beams subjected to, simultaneously, an axial load and moment has not been analytically studied. In this paper, we focus on developing analytical expressions to determine the first natural frequency of a thin-walled beam subjected to an axial load and end moment. Two problem-solving approaches are investigated; one is based on the root existence theorem and the other uses an energy method, in this case the Rayleigh method [22–24]. The paper shows the effects of several parameters, such as the geometry and the material properties of a beam, and the external loads on the value of the first natural frequency. In addition, the relationship between the vibration phenomenon and the stability of the beam is analyzed. The analytical expressions obtained in this study can be applied effectively for the optimization of tooth blade designs used in frame saw machines. The validity of these expressions is provided in comparison with results from ANSYS Mechanical APDL.

2. Mathematical Model and Solution Approach

The thin-walled beam investigated in this study has a rectangular cross section and length L subjected to an axial load F and moment M. $Oxyz$ is a global coordinate system, as shown in Figure 1, and $O\xi\eta\zeta$ is a local coordinate system attached to the deformed beam. u is the displacement of the elastic center along the x-direction and φ is the rotation angle. The displacement and the rotation angle of the cross-sections are assumed to be small.

The system of equations describing the beam deformation state is as follows [1, 2]:

$$\begin{cases} \mathrm{EI} \cdot \dfrac{\partial^4 u(z,t)}{\partial z^4} = M \cdot \dfrac{\partial^2 \varphi(z,t)}{\partial z^2} - F \cdot \dfrac{\partial^2 u(z,t)}{\partial z^2}, \\ \mathrm{GJ} \cdot \dfrac{\partial^2 \varphi(z,t)}{\partial z^2} = -M \cdot \dfrac{\partial^2 u(z,t)}{\partial z^2}, \end{cases} \tag{1}$$

where EI is the bending rigidity on the yz plane and GJ is the torsional rigidity.

In this study, we solve two problems of the beam with different boundary conditions, which are the simply supported-end and the laterally fixed-end conditions. The simply supported-end boundary condition is defined as follows [3]:

$$\begin{aligned} u = v = \varphi = 0, \quad & \text{at } z = \frac{-L}{2} \text{ and at } z = \frac{L}{2}, \\ \frac{\mathrm{d}^2 u}{\mathrm{d}z^2} = \frac{\mathrm{d}^2 v}{\mathrm{d}z^2} = \frac{\mathrm{d}^2 \varphi}{\mathrm{d}z^2} = 0, \quad & \text{at } z = \frac{-L}{2} \text{ and at } z = \frac{L}{2}. \end{aligned} \tag{2}$$

While the laterally fixed-end boundary condition is defined as shown below:

$$\begin{aligned} u = v = \varphi = 0, \quad & \text{at } z = \frac{-L}{2} \text{ and at } z = \frac{L}{2}, \\ \frac{\mathrm{d}u}{\mathrm{d}z} = \frac{\mathrm{d}\varphi}{\mathrm{d}z} = \frac{\mathrm{d}^2 v}{\mathrm{d}z^2} = 0, \quad & \text{at } z = \frac{-L}{2} \text{ and at } z = \frac{L}{2}. \end{aligned} \tag{3}$$

2.1. Approach 1: Based on the Root Existence Theorem. The flowchart used to determine the natural vibration frequencies is described in Figure 2. Considering the inertial

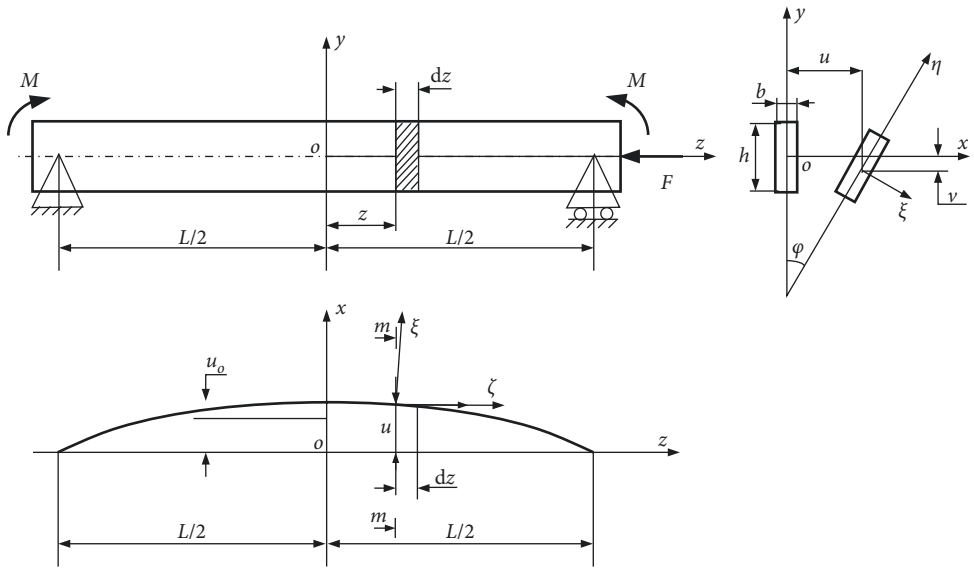

Figure 1: Thin-walled beam model.

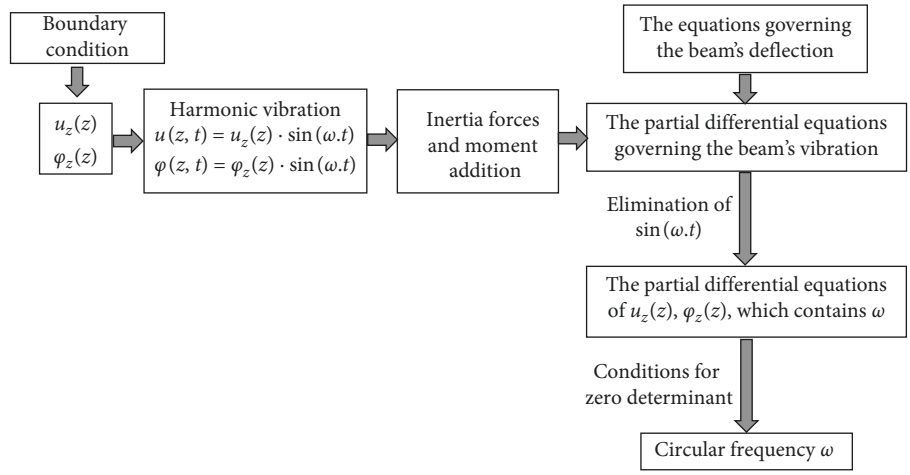

Figure 2: Flowchart to determine the free vibration frequencies by Approach 1.

forces and moment of the cross-section element in the system of equation (1), the partial differential equations governing the beam's vibration are

$$\begin{cases} \mathrm{EI} \cdot \dfrac{\partial^4 u(z,t)}{\partial z^4} + \rho bh \cdot \dfrac{\partial^2 u(z,t)}{\partial t^2} = M \cdot \dfrac{\partial^2 \varphi(z,t)}{\partial z^2} - F \cdot \dfrac{\partial^2 u(z,t)}{\partial z^2}, \\ \mathrm{GJ} \cdot \dfrac{\partial^2 \varphi(z,t)}{\partial z^2} - \rho \cdot I_p \cdot \dfrac{\partial^2 \varphi(z,t)}{\partial t^2} = -M \cdot \dfrac{\partial^2 u(z,t)}{\partial z^2}, \end{cases} \tag{4}$$

where ρ is the material density, h and b, respectively, denote the height and width of the cross section, and I_p is the polar moment of inertia. In a case of harmonic vibration, the displacement and rotation angle are represented as $u(z,t) = u_z(z) \cdot \sin(\omega t)$ and $\varphi(z,t) = \varphi_z(z) \cdot \sin(\omega t)$, respectively. Here, u_z is a function of z and ω is the circular natural frequency (radians per second). Substituting $u(z,t)$ and $\varphi(z,t)$ into (4) and canceling out the term $\sin(\omega t)$, the obtained system is as follows:

$$\begin{cases} \mathrm{EI} \cdot \dfrac{\partial^4 u_z(z)}{\partial z^4} - \omega^2 \cdot \rho bh \cdot u_z(z) = M \cdot \dfrac{\partial^2 \varphi_z(z)}{\partial z^2} - F \cdot \dfrac{\partial^2 u_z(z)}{\partial z^2}, \\ \mathrm{GJ} \cdot \dfrac{\partial^2 \varphi_z(z)}{\partial z^2} + \omega^2 \cdot \rho \cdot I_p \cdot \varphi_z(z) = -M \cdot \dfrac{\partial^2 u_z(z)}{\partial z^2}. \end{cases} \tag{5}$$

Considering the case of a simply supported beam, the selected asymptotic functions of u_z according to the boundary condition are $u_z = \varphi_z = 0$ and $u_z'' = \varphi_z'' = 0$ at the ends of $z = -L/2$ and $z = -L/2$. Thus, the displacement and rotation angle are estimated as follows:

$$u_z(z) = u_0 \cdot \cos\frac{\pi z}{L}, \tag{6}$$

$$\varphi_z(z) = \varphi_0 \cdot \cos\frac{\pi z}{L}. \tag{7}$$

Substituting u_z and φ_z into system (5) and canceling out the term $\cos(\pi z/L)$ results in the systems of u_0 and φ_0 as follows:

$$\begin{cases} u_0 \cdot \left[\mathrm{EI} \cdot \left(\frac{\pi}{L}\right)^4 - F \cdot \left(\frac{\pi}{L}\right)^2 - \omega^2 \cdot \rho \cdot b \cdot h\right] + \varphi_0 \cdot M \cdot \left(\frac{\pi}{L}\right)^2 = 0, \\ u_0 \cdot M \cdot \left(\frac{\pi}{L}\right)^2 + \varphi_0 \cdot \left[\mathrm{GJ} \cdot \left(\frac{\pi}{L}\right)^2 - \omega^2 \cdot \rho \cdot I_p\right] = 0. \end{cases} \tag{8}$$

Let $\omega_b^2 = (1/\rho bh) \cdot [\mathrm{EI} \cdot (\pi/L)^4 - F \cdot (\pi/L)^2]$ and $\omega_T^2 = GJ\pi^2/\rho I_p L^2$, yielding

$$\begin{cases} u_0 \cdot \left[\omega_b^2 - \omega^2\right] + \varphi_0 \cdot \dfrac{M\pi^2}{L^2\rho bh} = 0, \\ u_0 \cdot \dfrac{M\pi^2}{L^2\rho I_p} + \varphi_0 \cdot \left[\omega_T^2 - \omega^2\right] = 0. \end{cases} \tag{9}$$

According to the root existence theorem (u_0 and $\varphi_0 \neq 0$), the following determinant must be null:

$$\begin{vmatrix} \omega_b^2 - \omega^2 & \dfrac{M.\pi^2}{L^2\rho bh} \\ \dfrac{M.\pi^2}{L^2\rho I_p} & \omega_T^2 - \omega^2 \end{vmatrix} = 0. \tag{10}$$

This results in the following fourth-order equation:

$$\omega^4 - \left(\omega_b^2 + \omega_T^2\right) \cdot \omega^2 + \omega_b^2 \cdot \omega_T^2 - \frac{M^2\pi^4}{L^4\rho^2 I_p bh} = 0. \tag{11}$$

Let $\lambda = M^2\pi^4/L^4\rho^2 I_p bh$ and $\Delta = (\omega_b^2 + \omega_T^2)^2 - 4 \cdot (\omega_b^2\omega_T^2 - \lambda)$; to solve this equation, there are two roots as shown below:

$$\omega^2 = \frac{\left(\omega_b^2 + \omega_T^2\right) \pm \sqrt{\Delta}}{2}. \tag{12}$$

Here, the first natural frequency corresponds to the first vibration mode and is determined as follows:

$$\omega^2 = \frac{\left(\omega_b^2 + \omega_T^2\right) - \sqrt{\Delta}}{2}. \tag{13}$$

If $M = 0$ and the beam is subjected only to axial force F, then the first mode shape takes a purely bending form. The first natural frequency of the beam in this case is

$$\omega = \omega_b = \sqrt{\frac{1}{\rho bh} \cdot \left[EI \cdot \left(\frac{\pi}{L}\right)^4 - F \cdot \left(\frac{\pi}{L}\right)^2\right]}. \tag{14}$$

It is important to note that equation (14) is in good agreement with published results [3, 4].

2.2. Approach 2: Rayleigh Method. A flowchart of this approach is presented in Figure 3. Starting from the boundary conditions of the beam, the formula of u is derived. From system (1), we determine the formula of φ. It then becomes possible to derive the formulae of the strain energy U, the work caused by the external loads W, and the kinetic energy T. Based on the law of conservation of energy, the formula of the circular frequency ω is established. Next, the value of the circular frequency ω is defined.

Assuming that the beam vibration is harmonic, the displacement and the rotation angle can then be determined from $u(z,t) = u_z(z) \cdot \sin(\omega t)$ and $\varphi(z,t) = \varphi_z(z) \cdot \sin(\omega t)$, respectively. It is noteworthy that the formula of $\varphi_z(z)$ is defined by $u_z(z)$ on the basis of the boundary conditions and the following equation (from equation (1)):

$$\mathrm{GJ} \cdot \frac{\partial^2\varphi_z(z)}{\partial z^2} = -M \cdot \frac{\partial^2 u_z(z)}{\partial z^2}. \tag{15}$$

The strain energy of the system consists of two components; one is related to bending and the other is the torsion component, as follows:

$$U = \mathrm{EI} \cdot \int_0^{L/2} \left(\frac{\partial^2 u(z,t)}{\partial z^2}\right)^2 \mathrm{d}z + \mathrm{GJ} \cdot \int_0^{L/2} \left(\frac{\partial\varphi(z,t)}{\partial z}\right)^2 \mathrm{d}z. \tag{16}$$

On the contrary, the work caused by the moment M and axial load F is expressed as shown below [2]:

$$W = 2\int_0^{L/2} \left(M\frac{\partial^2 u(z,t)}{\partial z^2} \cdot \varphi(z,t)\right) \cdot \mathrm{d}z + F\int_0^{L/2} \left(\frac{\partial u(z,t)}{\partial z}\right)^2 \cdot \mathrm{d}z. \tag{17}$$

The complete potential energy of the system consists of U and W. Considering the load F as compressive, as shown in Figure 1, the value of the complete potential energy would be $U - W$. The complete potential energy would reach its maximum value as soon as the vibrating beam occupies its extreme position or when $\sin(\omega t) = 1$.

The kinetic energy T of the beam with a constant cross section consists of two components, in this case the component from the linear velocity and that related to the rotational velocity. The formula of T is [3]

$$T = \int_0^{L/2} \left\{\rho bh \cdot \left(\frac{\partial u(z,t)}{\partial t}\right)^2 + \rho I_p \left(\frac{\partial\varphi(z,t)}{\partial t}\right)^2\right\} \mathrm{d}z, \tag{18}$$

where ρbh is the linear density of the beam with a constant cross section.

Substituting $u(z,t) = u_z(z) \cdot \sin(\omega t)$ and $\varphi(z,t) = \varphi_z(z) \cdot \sin(\omega t)$ into (18) results in

$$T = \omega^2 \cdot \cos(\omega t)^2 \cdot \int_0^{L/2} \left[\rho bh \cdot u_z(z)^2 + \rho I_p \varphi_z(z)^2\right] \mathrm{d}z. \tag{19}$$

Let m be the modal (or generalized) mass of the beam, defined as follows:

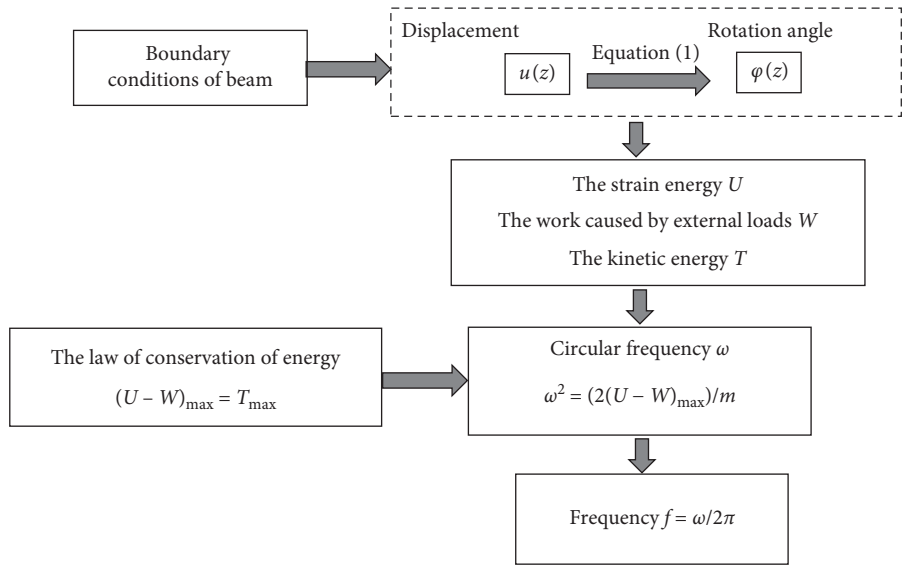

Figure 3: Flowchart to determine the free vibration frequencies by Approach 2.

$$m = 2\int_0^{L/2}\left(\rho bh \cdot u_z(z)^2 + \rho I_p \varphi_z(z)^2\right)\mathrm{d}z. \tag{20}$$

Here, the kinetic energy T is simplified to

$$T = \frac{1}{2}\omega^2 \cdot \cos(\omega t)^2 \cdot m. \tag{21}$$

Clearly, the kinetic energy would reach its maximum value as soon as the vibrating beam is in its middle position, i.e., $\cos(\omega t) = 0$. Assuming there are no energy losses, the equation of energy conservation is

$$(U - W)_{max} = T_{max}. \tag{22}$$

The first natural frequency of the system is then obtained as follows:

$$\omega^2 = \frac{2 \cdot (U - W)_{max}}{m}. \tag{23}$$

2.2.1. Beam with Simply Supported Ends. The displacement in this case according to equation (6) is represented as $u_z(z) = u_0 \cdot \cos(\pi z/L)$. Examining Figure 3 and expressions (15)–(23), the first natural frequency of the beam is

$$f = \frac{\omega}{2\pi} = \frac{1}{2}\cdot\sqrt{\frac{(\mathrm{EI}\cdot\mathrm{GJ}\cdot\pi^2 - \mathrm{GJ}\cdot FL^2 - L^2\cdot M^2)\cdot\mathrm{GJ}}{L^4\rho\left[bh(\mathrm{GJ})^2 + I_p M^2\right]}}. \tag{24}$$

If $M = 0$, equation (24) leads to expression (14), which in turn coincides with published results in the literature [3, 16, 20].

2.2.2. Beam with Laterally Fixed Ends. The displacement in accordance with the boundary condition $u(z) = u'(z) = 0$ at the ends $z = -L/2$ and $z = -L/2$ is formulated as follows:

$$u_z = \frac{u_0}{2}\cdot\left[1 + \cos\left(\frac{2\pi z}{L}\right)\right]. \tag{25}$$

From the flowchart given in Figure 3 and the expressions in equations (15)–(23), the first natural frequency of the beam is

$$f = \frac{\omega}{2\pi} = \sqrt{\frac{(4\cdot\mathrm{EI}\cdot\mathrm{GJ}\cdot\pi^2 - \mathrm{GJ}\cdot FL^2 - L^2M^2)\cdot\mathrm{GJ}}{3L^4\rho\cdot\left[(\mathrm{GJ})^2\cdot bh + I_p M^2\right]}}. \tag{26}$$

2.3. Stability of Thin-Walled Beams under Two External Loads. It is crucial to indicate that the expressions given in equations (24) and (26) can be applied not only to define the first natural frequency but also to establish the stability region based on equation $f = 0$ [1, 2]. Considering the case of a beam with simply supported ends, from equation (24), the expression describing the stability region of the beam under end moment M and axial load F is as follows:

$$\mathrm{EI}\cdot\mathrm{GJ}\cdot\pi^2 - \mathrm{GJ}\cdot FL^2 - L^2\cdot M^2 = 0. \tag{27}$$

If $M = 0$, from equation (27), the critical compressive load $F_{cr} = \pi^2\mathrm{EI}/L^2$, and if $F = 0$, the critical moment $M_{cr} = (\pi\sqrt{\mathrm{EI}\cdot\mathrm{GJ}})/L$. These results are in good agreement with previously published findings [1, 2, 25].

Meanwhile, for a beam with laterally fixed ends, from equation (26), the expression describing the stability region of the beam is

$$4\cdot\mathrm{EI}\cdot\mathrm{GJ}\cdot\pi^2 - \mathrm{GJ}\cdot FL^2 - L^2\cdot M^2 = 0. \tag{28}$$

When $M = 0$ and $F = 0$, from equation (27), there are the critical compressive load $F_{cr} = 4\pi^2\mathrm{EI}/L^2$ and the critical moment $M_{cr} = (2\pi\sqrt{\mathrm{EI}\cdot\mathrm{GJ}})/L$, which are also in good agreement with previously published results [25].

3. Application to the Vibration and Stability Analyses of Saw Blades

The application of the explicit analytical expressions developed above to the vibration and stability analyses of tooth blades is presented in this section. These analyses construct a firm basis for the optimization of an innovative frame saw machine design, as described in the literature [5]. The experimental mock-up of this machine, shown in Figure 4(a), reveals that in order to have an optimal design, a number of technical requirements must be considered simultaneously [5]. Apart from the main criteria, including the durability, hardness, and stability, it is important to avoid the resonance of saw tooth blades [26]. Resonant oscillation may cause the blade structures to break, as shown in Figure 4(b). Indeed, this is the greatest barrier when attempting to increase the speed of frame saw machines, leading to productivity limitations.

Prokopov [26] found that there are several mode shapes of blade vibration, as presented in Figure 5. Among them, the most severe cases of coupled bending and torsional deformations should be examined because the frequency of these types of vibration is close to that of the machine shaft. Thus, resonance occurs when the vibration frequency of the machine shaft attains the value of the first natural frequency. However, in the literature [26], there is lack of information about the relationships between the vibration frequency and the blade parameters. What does exist is insufficient to establish mathematical models for the optimal design of a frame saw machine.

In fact, the blade must be steady while operating; thus, during the assembly process, it is often stretched with a preload, F_0. This load is placed toward the tooth side at distance e from the blade axle, as illustrated in Figure 6. Therefore, the saw blade (or thin-walled beam) is actually subjected to load F_0 and moment $M = F \cdot e$. Substituting $M = -F_0 \cdot e$ and $F_0 = -F$ equations (24) and (26), the first natural frequency of the blade can be determined appropriately.

For a saw blade with the simply supported ends, equation (24) results in

$$f = \frac{1}{2} \cdot \sqrt{\frac{\left(\mathrm{EI} \cdot \mathrm{GJ}\pi^2 + \mathrm{GJ} \cdot F_0 L^2 - L^2 F_0^2 e^2\right) \cdot \mathrm{GJ}}{L^4 \rho \left[bh\,(\mathrm{GJ})^2 + I_p F_0^2 e^2\right]}}, \tag{29}$$

and for a saw blade with the laterally fixed ends, from equation (26) the natural frequency is

$$f = \sqrt{\frac{\left(4\mathrm{EI} \cdot \mathrm{GJ}\pi^2 + \mathrm{GJ} \cdot F_0 L^2 - L^2 F_0^2 e^2\right) \cdot \mathrm{GJ}}{3L^4 \rho \left[bh\,(\mathrm{GJ})^2 + I_p F_0^2 e^2\right]}}. \tag{30}$$

When $f = 0$, from equations (29) and (30), the expression describing the stability region of the saw blade can be obtained in a straightforward manner in the space of F_0 and e with various boundary conditions. For the boundary conditions of simply supported ends and laterally fixed ends, from equations (29) and (30), the corresponding expressions are presented in

$$\mathrm{EI} \cdot \mathrm{GJ}\pi^2 + \mathrm{GJ} \cdot F_0 L^2 - L^2 F_0^2 e^2 = 0, \tag{31}$$

$$4\mathrm{EI} \cdot \mathrm{GJ}\pi^2 + \mathrm{GJ} \cdot F_0 L^2 - L^2 F_0^2 e^2 = 0. \tag{32}$$

Equations (29) and (30) are very useful for the optimization of an innovative frame saw machine design while considering the stability and resonance problems [27].

4. Results of Validations and Discussion

This section serves to validate the analytical expressions obtained from the two approaches. The results are compared with the numerical data obtained from the FEM software ANSYS Mechanical APDL. In order to represent conveniently the results in tables and 2D graphs, the set of values of (F_0, e) is used instead of (F, M). It should be noted that (F_0, e) must be selected to ensure that the system is stable, as described above in Section 2.3. For instance, for a beam with simply supported ends subjected to an eccentric load, the boundary of the stability region is a second-order equation of F_0, in this case $\mathrm{EI} \cdot \mathrm{GJ}\pi^2 + \mathrm{GJ} \cdot F_0 L^2 - L^2 F_0^2 e^2 = 0$. Hence, for every value of e, there is a corresponding critical value of F_0. The validation is carried out for the case of a steel thin-walled beam with a rectangular cross section. The input data of the beam are as follows: length $L = 0.8$ (m), height $h = 0.06$ (m), width $b = 0.003$ (m), $E = 2{\cdot}10^{11}$ (N/m^2), a Poisson's ratio $\mu = 0.28$, and density $\rho = 7850$ (kg/m^3). The natural frequencies obtained by expressions (13) and (29) on the basis of the two approaches are shown in Table 1. The eccentricity e varies from 0 to $2h$, while the load F_0 ranges from −200 N to 1600 N. The negative load F_0 indicates that the beam is under compression. The analytical results show that there is no discrepancy between the two approaches. The expressions in equations (29) and (30) from Approach 2 are chosen for a comparison with the results from the ANSYS Mechanical APDL software.

4.1. Beam with Simply Supported Ends. For this boundary condition, the beam is modelled in the FEM software, as shown in Figure 7. The 3D graph in Figure 8 illustrates the relationship between the first natural frequency of the beam and the set (F_0, e). The comparison of the results from Approach 2 and the FEM software can be observed in Figure 9 and Table 2, which show that the differences between the results from these two methods are within 3%, which is regarded as minor. The maximum is 2.7% when $F_0 = -200$ N and $e = 0$ mm. It is essential to point out that the first natural frequency f is proportional to the load F_0 and disproportional to the eccentricity e. This statement is in agreement with findings in the literature [3, 20].

4.2. Beam with Laterally Fixed Ends. Similarly, a FEM model of the beam with laterally fixed ends is illustrated in Figure 10. The first natural frequency f of the beam with the laterally fixed ends in the parameter space of F_0 and e

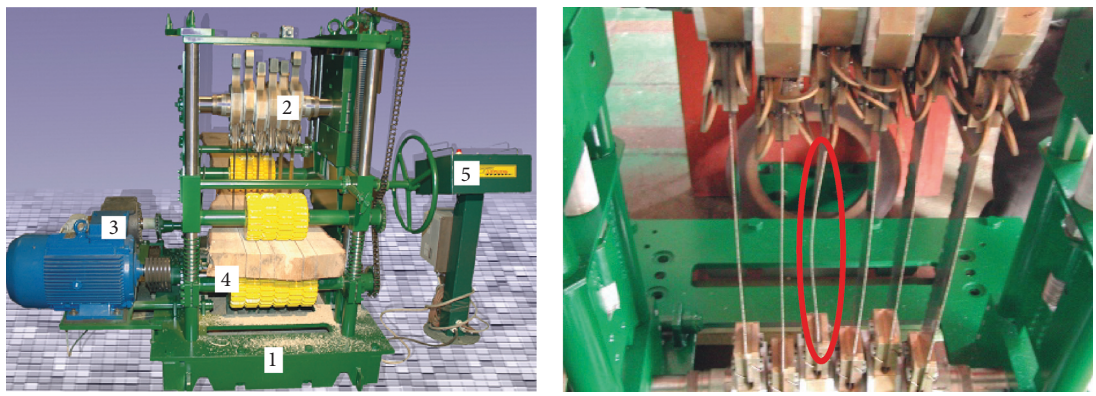

(a) (b)

Figure 4: The frame saw machine in the experiment and resonant oscillation of the tooth blade: (a) frame saw machine in the experiment and (b) resonant oscillation causing breakage of a blade structure.

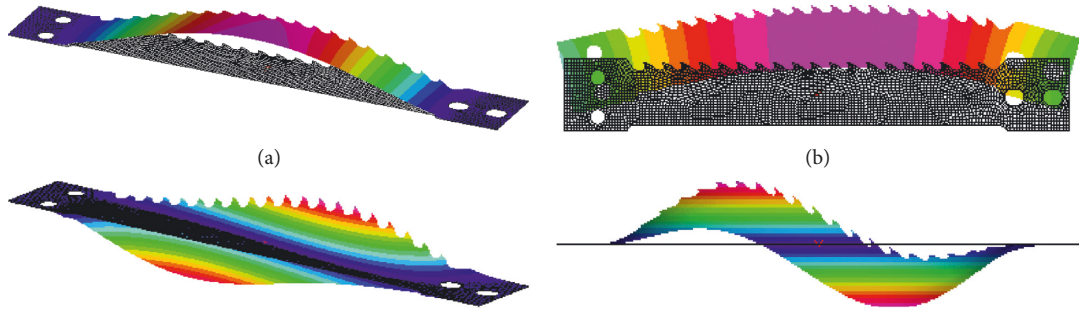

(a) (b) (c) (d)

Figure 5: Natural vibration type of the tooth blade: (a) type 1, bending; (b) type 2, bending; (c) type 3, twist bending; (d) type 4, two span twist bending.

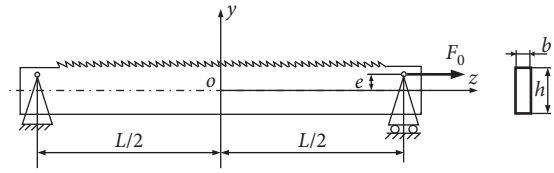

Figure 6: Model of the saw blade under an eccentric load.

Table 1: Natural frequency f of the beam with the simply supported ends by Approach 1 and Approach 2.

E		0			h			$2h$	
F_0	App. 1 equation (13)	App. 2 equation (29)	Dev. (%)	App. 1 equation (13)	App. 2 equation (29)	Dev. (%)	App. 1 equation (13)	App. 2 equation (29)	Dev. (%)
−200	7.73	7.73	0.00	7.67	7.67	0.00	7.49	7.49	0.00
0	10.73	10.73	0.00	10.73	10.73	0.00	10.73	10.73	0.00
200	13.05	13.05	0.00	13.02	13.02	0.00	12.91	12.91	0.00
400	15.02	15.02	0.00	14.90	14.90	0.00	14.51	14.51	0.00
600	16.76	16.76	0.00	16.51	16.51	0.00	15.71	15.71	0.00
800	18.34	18.34	0.00	17.92	17.92	0.00	16.60	16.60	0.00
1000	19.79	19.79	0.00	19.18	19.18	0.00	17.22	17.22	0.00
1200	21.14	21.14	0.00	20.31	20.31	0.00	17.60	17.60	0.00
1400	22.41	22.41	0.00	21.34	21.34	0.00	17.77	17.77	0.00
1600	23.61	23.61	0.00	22.28	22.28	0.00	17.72	17.72	0.00

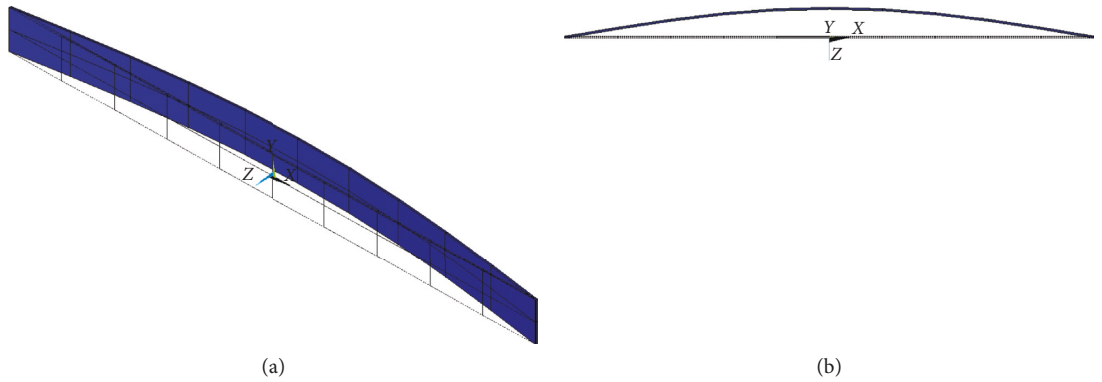

(a) (b)

Figure 7: FEM model of a thin-walled beam with simply supported ends in ANSYS mechanical APDL: (a) 3D view and (b) top view.

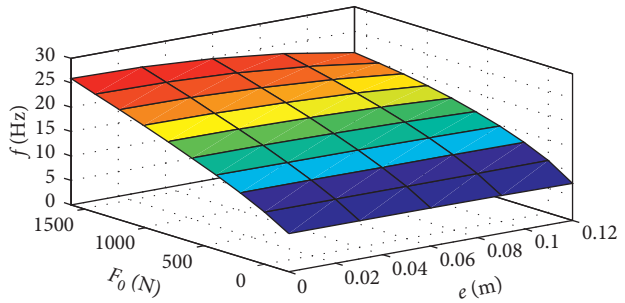

Figure 8: Natural frequency f of the beam with simply supported ends in the parameter space of F_0 and e in accordance with equation (29).

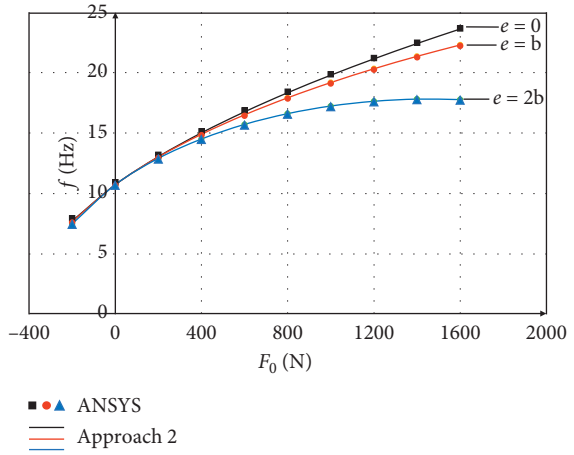

Figure 9: Natural frequency with respect to different values of F_0 and e for the beam with simply supported ends by ANSYS Mechanical APDL and Approach 2 (equation (29)).

Table 2: Natural frequency f of the beam with simply supported ends by ANSYS mechanical APDL and Approach 2 (equation (29)).

e	0			h			$2h$		
F_0	APDL	App. 2 equation (29)	Dev. (%)	APDL	App. 2 equation (29)	Dev. (%)	APDL	App. 2 equation (29)	Dev. (%)
−200	7.95	7.73	2.77	7.61	7.67	0.76	7.44	7.49	0.63
0	10.94	10.73	1.97	10.68	10.73	0.50	10.68	10.73	0.45
200	13.22	13.05	1.28	12.96	13.02	0.46	12.85	12.91	0.41
400	15.16	15.02	0.91	14.84	14.90	0.36	14.46	14.51	0.35
600	16.88	16.76	0.70	16.45	16.51	0.35	15.66	15.71	0.34
800	18.44	18.34	0.55	17.86	17.92	0.31	16.55	16.60	0.30
1000	19.88	19.79	0.44	19.12	19.18	0.31	17.18	17.22	0.25
1200	21.22	21.14	0.36	20.25	20.31	0.29	17.57	17.60	0.19
1400	22.48	22.41	0.30	21.28	21.34	0.26	17.75	17.77	0.11
1600	23.67	23.61	0.25	22.22	22.28	0.25	17.72	17.72	0.01

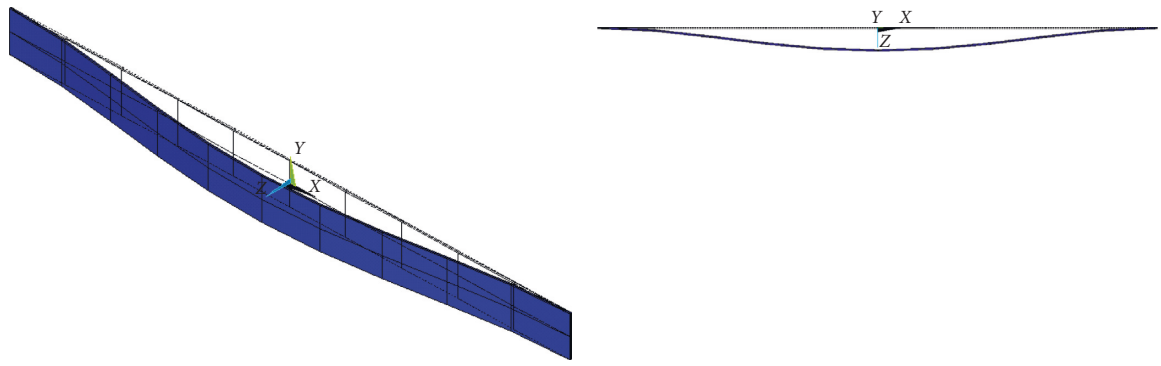

(a) (b)

Figure 10: FEM model of the thin-walled beam with laterally fixed ends in ANSYS APDL: (a) 3D view and (b) top view.

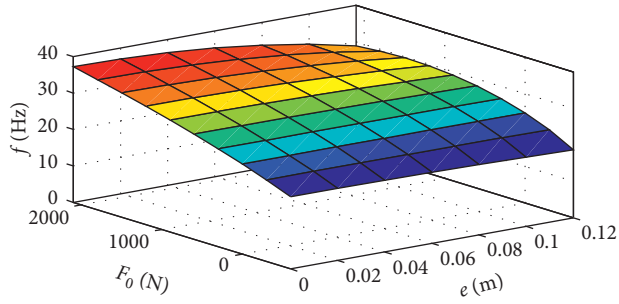

Figure 11: Natural frequency f of the beam with laterally fixed ends in the parameter space of F_0 and e in accordance with equation (30).

Table 3: Natural frequency f of the beam with laterally fixed ends by ANSYS mechanical APDL and Approach 2.

e	0			h			$2h$		
F_0	APDL	App. 2 equation (30)	Dev. (%)	APDL	App. 2 equation (30)	Dev. (%)	APDL	App. 2 equation (30)	Dev. (%)
−600	19.94	19.82	0.61	19.66	19.53	0.68	18.81	18.63	0.93
−300	22.41	22.43	0.12	22.35	22.37	0.11	22.16	22.18	0.06
0	24.61	24.78	0.67	24.61	24.78	0.67	24.61	24.78	0.67
300	26.62	26.92	1.12	26.57	26.86	1.10	26.42	26.70	1.07
600	28.47	28.90	1.50	28.29	28.70	1.45	27.72	28.09	1.34
900	30.20	30.75	1.83	29.81	30.33	1.74	28.59	29.02	1.49
1200	31.82	32.50	2.13	31.16	31.78	1.99	29.08	29.53	1.56
1500	33.36	34.16	2.40	32.37	33.08	2.19	29.20	29.65	1.52
1800	34.82	35.74	2.65	33.46	34.25	2.36	28.97	29.38	1.39
2100	36.21	37.26	2.88	34.43	35.30	2.50	28.39	28.71	1.14

in accordance with equation (30) is shown in Figure 11. The first natural frequency of the beam derived from the FEM software and equation (30) is presented in Table 3 and Figure 12, which indicate that the results in this case are less precise than the previous outcome. The result would be more exact if the formula of the deflection curve u had been estimated accurately. The data from Table 3 and Figure 12 imply that the Rayleigh quotient tends to overestimate the natural frequency of the beam, i.e., it provides an upper bound of the exact solution, which coincides with the pertinent theory [3]. In addition, the accuracy of the expressions in equations (26) and (30) could be improved if Ritz's method is used. However, the resultant expressions would be cumbersome and complex. Therefore, they are not presented in this paper for brevity.

In general, for both cases the differences are marginal (less than 3%). Thus, the explicit analytical expressions can be used conveniently in practice for the optimized designs of thin-walled beams.

5. Conclusion

In this study, the first natural frequencies of thin-walled beams were determined by two approaches: one based on the root existence theorem of a differential equation system and the other on the Rayleigh method. The first approach can only be used for the boundary condition of simply supported ends, while the second can be applied to various conditions. From these two approaches, the analytical expressions to define the first natural frequencies of a beam with simply

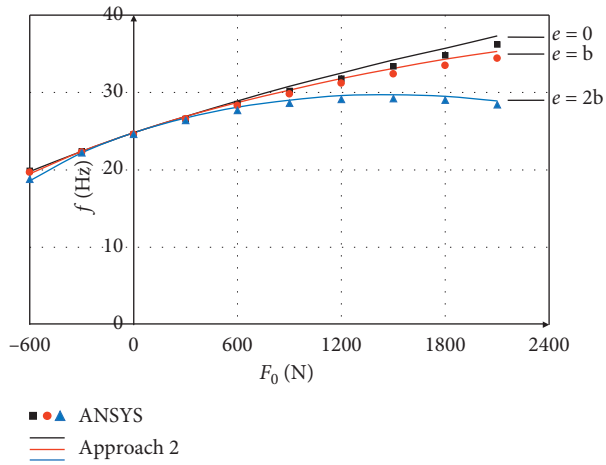

Figure 12: The first natural frequency with respect to different values of F_0 and e for the beam with laterally fixed ends by ANSYS APDL and Approach 2 (equation (30)).

supported ends or laterally fixed ends were derived. The two approaches yielded identical results. Moreover, in a comparison with the numerical results from the FEM software ANSYS Mechanical APDL, the differences were found to be minor, i.e., less than 3%. The obtained explicit expressions can be applied in a straightforward manner to analyze the vibration and stability of tooth blades in frame saw machines. Moreover, the results are useful for the optimization of regular thin-walled beam structures in general.

Data Availability

The data used to support the findings of this study are available from the corresponding author upon request.

Conflicts of Interest

The authors declare that there are no conflicts of interest regarding the publication of this paper.

Acknowledgments

This research was funded by Vietnam National Foundation for Science and Technology Development (NAFOSTED) under grant no. 107.01-2019.14. The authors would like to express the gratitude to the scientists and colleagues at Le Quy Don Technical University, Industrial University of Ho Chi Minh, and Ton Duc Thang University, Vietnam, for the interest and invaluable contributions to the paper

References

[1] V. B. Phung, H. M. Dang, S. S. Gavriushin, and V. D. Nguyen, "Boundary of stability region of a thin-walled beam under complex loading condition," *International Journal of Mechanical Sciences*, vol. 122, pp. 355–361, 2017.

[2] V. B. Phung, V. D. Nguyen, V. S. Prokopov, and H. M. Dang, "Improved generalized procedure for determining critical state of a thin-walled beam under combined symmetric load," *International Journal of Structural Stability and Dynamics*, vol. 19, no. 8, Article ID 1950098, 2019.

[3] S. Timoshenko, *Vibration Problems in Engineering*, Wiley-Interscience, New York, NY, USA, 1964.

[4] V. Z. Vlasov, *Thin Walled Elastic Beams*, Israel Program for Scientific Transactions, Jerusalem, Israel, 1961.

[5] V. B. Phung, *Automation and management of the decision-making process for multi-criteria design of the saw unit of a multirip bench*, Ph.D. dissertation, Bauman Moscow State Technical University, Moscow, Russia, 2017.

[6] J. Li, R. Shen, H. Hua, and X. Jin, "Coupled bending and torsional vibration of axially loaded thin-walled Timoshenko beams," *International Journal of Mechanical Sciences*, vol. 46, no. 2, pp. 299–320, 2004.

[7] J. Li, W. Li, R. Shen, and H. Hua, "Coupled bending and torsional vibration of nonsymmetrical axially loaded thin-walled Bernoulli–Euler beams," *Mechanics Research Communications*, vol. 31, no. 6, pp. 697–711, 2004.

[8] J. R. Banerjee, "Coupled bending-torsional dynamic stiffness matrix for beam elements," *International Journal for Numerical Methods in Engineering*, vol. 28, no. 6, pp. 1283–1298, 1989.

[9] J. R. Banerjee and F. W. Williams, "Coupled bending-torsional dynamic stiffness matrix of an axially loaded Timoshenko beam element," *International Journal of Solids and Structures*, vol. 31, no. 6, pp. 749–762, 1994.

[10] G. M. Vörös, "On coupled bending-torsional vibrations of beams with initial loads," *Mechanics Research Communications*, vol. 36, no. 5, pp. 603–611, 2009.

[11] M. T. T. Kashani, S. Jayasinghe, and S. M. Hashemi, "On the flexural-torsional vibration and stability of beams subjected to axial load and end moment," *Shock and Vibration*, vol. 2014, Article ID 153532, 11 pages, 2014.

[12] S. P. Machado and V. H. Cortínez, "Free vibration of thin-walled composite beams with static initial stresses and deformations," *Engineering Structures*, vol. 29, no. 3, pp. 372–382, 2007.

[13] T. P. Vo and J. Lee, "Interaction curves for vibration and buckling of thin-walled composite box beams under axial loads and end moments," *Applied Mathematical Modelling*, vol. 34, no. 10, pp. 3142–3157, 2010.

[14] Y. Toyota, T. Hirose, S. Ono, and K. Shidara, "Experimental study on vibration characteristics of prestressed concrete beam," *Procedia Engineering*, vol. 171, pp. 1165–1172, 2017.

[15] A. Bokaian, "Natural frequencies of beams under tensile axial loads," *Journal of Sound and Vibration*, vol. 142, no. 3, pp. 481–498, 1990.

[16] H. Abramovich, "Natural frequencies of Timoshenko beams under compressive axial loads," *Journal of Sound and Vibration*, vol. 157, no. 1, pp. 183–189, 1992.

[17] B. Binici, "Vibration of beams with multiple open cracks subjected to axial force," *Journal of Sound and Vibration*, vol. 287, no. 1-2, pp. 277–295, 2005.

[18] W. Busool and M. Eisenberger, "Vibrations of axially loaded continuous beams," *International Journal of Structural Stability and Dynamics*, vol. 2, no. 1, pp. 117–133, 2002.

[19] B. Béri, G. Stépán, and S. J. Hogan, "Effect of potential energy variation on the natural frequency of an Euler-Bernoulli cantilever beam under lateral force and compression," *Journal of Applied Mechanics*, vol. 84, no. 5, pp. 1–8, 2017.

[20] S. Suryanarayan and A. Joshi, "Coupled flexural torsional vibration of an eccentrically stretched strip," *Journal of Applied Mechanics*, vol. 49, no. 3, pp. 669–671, 1982.

[21] E. Dokumaci, "An exact solution for coupled bending and torsion vibrations of uniform beams having single cross-

sectional symmetry," *Journal of Sound and Vibration*, vol. 119, no. 3, pp. 443–449, 1987.

[22] A. Mirzabeigy, V. Dabbagh, and R. Madoliat, "Explicit formulation for natural frequencies of double-beam system with arbitrary boundary conditions," *Journal of Mechanical Science and Technology*, vol. 31, no. 2, pp. 515–521, 2017.

[23] R. R. Craig and A. J. Kurdila, *Fundamental of Structural Dynamics*, Wiley, Hoboken, NJ, USA, 2nd edition, 2006.

[24] H. Ozbasaran, "Convergence of the Rayleigh–Ritz method for buckling analysis of arbitrarily configured I-section beam–columns," *Archive of Applied Mechanics*, vol. 89, no. 12, pp. 2397–2414, 2019.

[25] S. Timoshenko and J. M. Gere, *Theory of Elastic Stability*, McGraw-Hill, New York, NY, USA, 2nd edition, 1961.

[26] V. S. Prokopov, *Development of methods for the numerical analysis of the dynamic characteristics of a multi-saw machine with circular translational motion of sawblades*, Bauman Moscow State Technical University, Moscow, Russia, Ph.D. dissertation, 2013.

[27] H. M. Dang, V. B. Phung, and V. D. Nguyen, "Multi-objective design for a new type of frame saw machine," *International Journal of Mechanical and Production Engineering Research and Development*, vol. 9, no. 2, pp. 449–466, 2019.